

# Precision Hadron Physics at the Mainz Microtron MAMI and MESA \*

Achim G. Denig<sup>1,1)</sup>

<sup>1</sup> Institute for Nuclear Physics and PRISMA Cluster of Excellence,  
Johannes Gutenberg University Mainz, 55099 Mainz, Germany

**Abstract:** The Mainz Microtron MAMI is a high-intensity electron accelerator for fixed-target experiments in the fields of hadron and low-energy particle physics. It provides a polarized beam of up to 1.6 GeV beam energy. Two major installations are currently in operation at MAMI: the high-resolution spectrometer setup A1 as well as the A2 detector setup, which consists of the Crystal Ball detector in conjunction with the TAPS calorimeter. Highlights of the research program at MAMI are measurements of the electromagnetic form factors and polarizabilities of the proton, which are related to the proton radius puzzle, the measurement of the transition form factors and slope parameters of the eta meson, as well as the search for hypothetical gauge bosons of the dark sector, also denoted as dark photons. Currently, the new electron accelerator MESA is in preparation at Mainz, which will allow for a precision measurement of the electroweak mixing angle at low momentum transfer as well as measurements of low-energy electron-nucleon/nucleus scattering for various applications in nuclear, hadron, and particle physics.

**Key words:** Hadron physics, electron scattering, electromagnetic form factors, polarizability, meson decays, proton radius, electroweak mixing angle, dark photon

**PACS:** 13.40.Gp, 14.40.Be, 14.80.Va

## 1 The MAMI and MESA facilities

### 1.1 The MAMI facility

The Mainz Microtron MAMI is a continuous-wave (CW), fixed-target electron accelerator for beam energies of up to 1.604 GeV [1]. It is operated as a University accelerator by the Institute for Nuclear Physics of the Johannes Gutenberg University (JGU) of Mainz. MAMI is constructed as a cascade of four microtrons, of which the last stage, the harmonic double-sided microtron MAMI-C, represents a new concept in microtron accelerator technology. The beam intensity (up to  $\approx 100 \mu\text{A}$ ), the beam polarization (up to 85%), and the energy resolution (0.1 MeV) are among the highest in the world. Also the availability of the accelerator, which is routinely operated by students, is very high with approximately 7000 hours of beam delivered for the users per year. Currently, two major installations are operated at MAMI, the electron scattering experiment A1 as well as the A2 experiment at the tagged photon beam facility.

#### 1.1.1 The A1 electron scattering experiment

The A1 experiment consists of three high-resolution magnetic spectrometers, allowing for coincidence electron scattering experiments [2]. The spectrometers with a weight of 300 tons each, can be rotated around a common pivot. They have a maximum momentum coverage of up to 870 MeV/c, spatial acceptances of 28 msr and

an outstanding momentum resolution of  $10^{-4}$ . The focal planes of the spectrometers comprise drift chambers, scintillators as timing detectors, Cherenkov detectors, and a proton polarimeter. In addition, a compact spectrometer (KAOS) for the detection of kaons is available. At present, a highly segmented large solid angle neutron detector is under construction. High-power cryogenic targets for liquid hydrogen and deuterium, pressurized  $^3\text{He}$  and  $^4\text{He}$  as well as a polarized  $^3\text{He}$  target are available as well.

#### 1.1.2 The A2 photon scattering setup

The A2 collaboration runs a facility for energy tagging of bremsstrahlung photons [3]. An additional end point tagger was built to cover the high-energy part of the photon energy spectrum and to access the  $\eta'$  threshold. The primary detector arrangement consists of the Crystal Ball and TAPS detectors. This setup is particularly suitable for the detection of photons with a solid angle of almost  $4\pi$  with high resolution and high count rate capabilities. A set of two inner multiwire proportional chambers and a barrel of scintillation detectors serve for tracking and particle identification. A recoil proton polarimeter is also available. A polarized frozen-spin target for protons and deuterons with longitudinal and transverse polarization is operating successfully [4]. Very high relaxation times of up to 3000 hours have been obtained.

Received 14 Sep. 2014

\* Supported by the Collaborative Research Centre CRC 1044

1) E-mail: denig@kph.uni-mainz.de

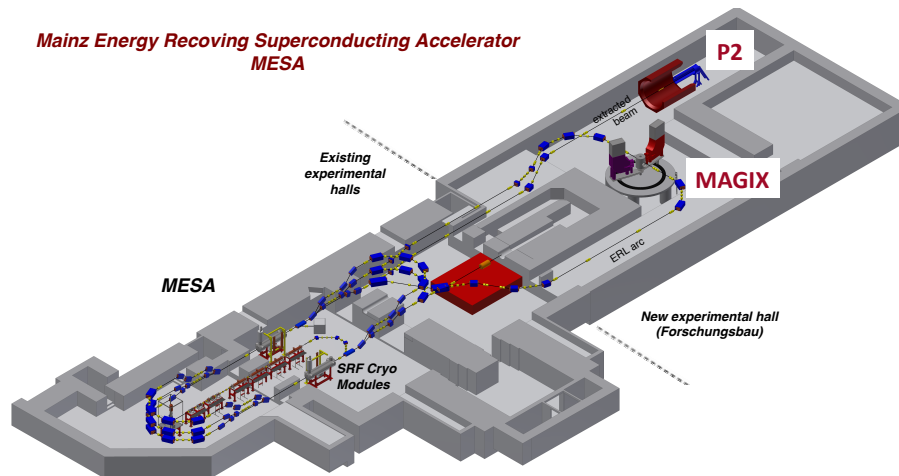


Fig. 1. The future MESA accelerator facility with the accelerator itself (left) and the two experiments P2 and MAGIX (right).

## 1.2 The future MESA facility

In addition to MAMI, a new accelerator, the Mainz Energy Recovering Superconducting Accelerator (MESA), a compact CW linear accelerator using superconducting cavities and the energy-recovering linac (ERL) concept [5], is currently under construction at Mainz, see Fig. 1. It will be housed in existing underground halls as well as a new hall and will run in parallel to MAMI. MESA exhibits a beam energy of maximum 155 MeV, however with beam intensities (at least 1 mA) which exceed the intensities achieved at MAMI by more than one order of magnitude when running in the ERL mode. The commissioning of the MESA accelerator as well as the experiments P2 (operated in the extracted beam mode) and MAGIX (an internal target experiment for the ERL mode) is foreseen for 2019. The MESA beam can be polarized both in the external as well as the ERL operation mode.

### 1.2.1 The P2 experiment

The major goal of the P2 experiment is a new precision measurement of the electroweak mixing angle,  $\sin^2\Theta_W$  at low momentum transfer. The P2 experiment is described in detail in a dedicated contribution to these proceedings, see Ref. [6]. A measurement of this kind has the potential to probe New Physics scenarios at a mass scale of up to 49 TeV, being hence complementary to searches for New Physics at the Large Hadron Collider. The P2 experiment might also be used for a measurement of the neutron skin of nuclei with important implications for astrophysics and a detailed understanding of neutron stars.

### 1.2.2 The MAGIX experiment

The operation of a high-intensity ERL beam with intensities of at least 1 mA in conjunction with an internal gas target is a novel experimental approach and will

yield competitive luminosities of  $10^{35} \text{ cm}^{-2}\text{s}^{-1}$ . To fully exploit the physics opportunities of such a setup, the MAGIX high-resolution double-arm spectrometers will be constructed. MAGIX will allow to continue the search for a hypothetical gauge boson  $\gamma'$  (dark photon), which is predicted in the context of dark matter models. Furthermore, precision measurements of the electromagnetic form factors of the nucleon at low momentum transfers will be possible at MAGIX, as motivated by the proton radius puzzle. The MAGIX spectrometers will be equipped with large area GEM-based focal plane detectors. For the internal target, a supersonic gas jet target as well as a T-shaped target with the option of target polarization are prepared.

## 2 Experiments related to the Proton Radius Puzzle

The charge radius of the proton currently is determined using different methods [8]: (i) by measuring the electromagnetic form factor of the proton in electron-proton scattering experiments at low momentum transfer; (ii) by measuring various atomic transitions in hydrogen; (iii) by measuring the lamb shift of the  $2S-2P$  transition in muonic hydrogen. The latter method comes out to provide an extremely precise determination of the proton radius on the permille level. It however shows a dramatic difference with respect to the first two methods, which themselves are consistent with each other and provide measurements on the percent level. This surprising situation was dubbed the proton radius puzzle. It has triggered in the past years a large number of theoretical investigations, which have tried to explain the discrepancy by unaccounted hadronic uncertainties in the muonic hydrogen measurement. In the meantime, there is however consensus in the community that the hadronic

correction associated with the two-photon exchange diagram represents by far the largest hadronic correction [7]. Nonetheless, it, amounts to only about 10% of the total discrepancy, and, furthermore, is known with approximately 10% accuracy and therefore by no means can be the sole reason for the proton radius puzzle. There are speculations whether the proton radius puzzle might indicated physics beyond the Standard Model of particle physics. Before coming to this conclusions, the experiments both in electron-proton scattering as in electronic and muonic atomic spectroscopy need to be scrutinized.

The most precise measurement of the proton radius according to method (i) has been performed at A1/MAMI [9]. A momentum range of as low as few  $10^{-3}$   $\text{GeV}^2$  has been covered, yielding a proton radius of  $\langle r \rangle = 0.879(8)$  fm. This deviates by approximately 7 standard deviations from the muonic hydrogen value, obtained at PSI with  $\langle r \rangle = 0.8409(4)$  fm [10]. It has been speculated whether the momentum range covered by A1 might not be low enough for a precise determination of the proton radius as an extrapolation to essentially zero momentum transfer has to be made [11] (see also the reply in Ref.[12] to this criticism). In the following, we present two new approaches to achieve extremely low ranges of momentum transfer, either by utilizing the method of initial state radiation, or, by carrying out dedicated measurements at the low-energy facility MESA.

## 2.1 Initial State Radiation Measurement at A1

The radiation of a high-energetic photon from the incoming electron, involved in the electron-proton scattering process, leads to a reduction of the effective momentum transfer probing the proton. In fact, for a given setup of beam energies and polar angles of the A1 spectrometers, values of momentum transfer down to  $2 \cdot 10^{-4}$   $\text{GeV}^2$  can be probed. The method of course needs a good theoretical understanding of the effects of final state radiation, or of the radiation of photons from the protons. While the former is a pure QED process and is therefore known precisely, the latter requires an a priori knowledge of the electromagnetic form factors of the proton, which shall be measured. The present accuracy of the form factor measurements is however sufficient for the purpose of subtracting this background process.

At A1/MAMI, data at beam energies of 495 MeV, 330 MeV, and 195 MeV has been taken. The analysis of the data is currently ongoing. Preliminary results can be seen for the two higher energy points in Fig. 2. In the upper panel the counting rate for the two energy settings is shown, along with the background expected from inelastic processes. Both the data spectrum and the detector simulation are shown as a function of the energy of the electron in the final state. A very good agreement between data and simulation on the sub-percent level is

found, as displayed in the lower panel. The main limitation is presently given by the systematic effects associated with the background from the target walls. The current results indicate that a precision measurement with a competitive accuracy of the low-momentum region can be carried out with the initial state radiation method.

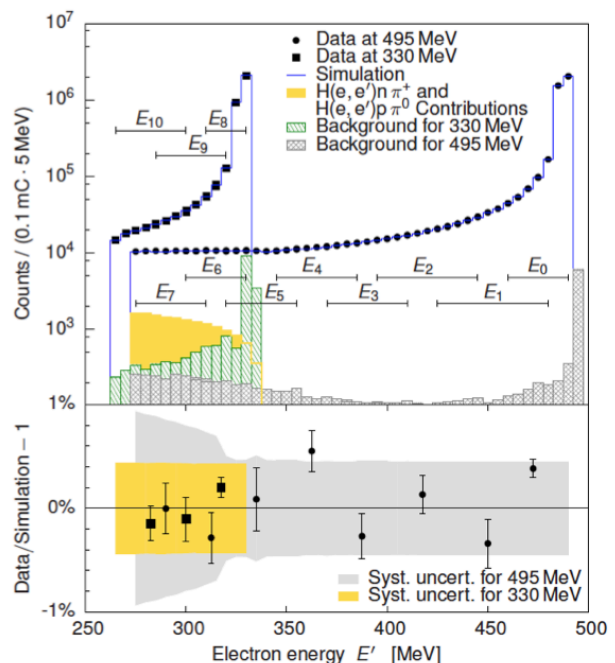


Fig. 2. Initial state radiation analysis of the elastic process  $ep \rightarrow e'p'$ . See text for explanations.

## 2.2 Future Opportunities at MAGIX/MESA

The low beam energy of MESA in combination with the high resolution of the MAGIX double arm spectrometer setup will be ideal for the measurement of electromagnetic form factors at low momentum transfer. It will also be possible to measure the ratio of the electric to the magnetic form factors,  $\mu_p G_E/G_M$ , using the double polarization method, developed at BLAST/MIT-Bates. A simulation has been carried out, assuming a polarized MESA beam (1 mA beam current), along with a target polarization of 80% (target density  $3 \cdot 10^{15}/\text{cm}^2$  as in the BLAST target). Fig.3 shows the results of the simulation with the projected error bars of the MAGIX measurement (red points), together with the currently existing world data set. The high accuracy of the data and the fact that a low momentum transfer can be achieved, will lead to new insights regarding the structure of the nucleon.

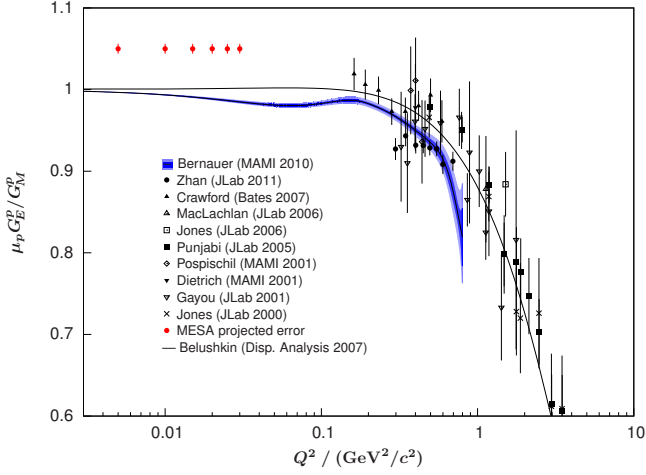


Fig. 3. Ratio of the electric to the magnetic form factor,  $\mu_p G_E^p / G_M^p$ , as a function of momentum transfer: projected error bars of the future measurement at MAGIX (red data points) from a simulation, assuming a polarized MESA beam and target. Shown is also the currently existing world data set of this ratio.

### 3 Investigations of Proton and Meson Structure using tagged Photons

#### 3.1 Proton Polarizabilities at A2

As mentioned above, the largest uncertainty for the determination of the proton radius from the muonic hydrogen lamb shift measurement arises from the two-photon exchange diagram. This effect can be related to the forward Compton scattering amplitude, which in turn is related to the magnetic polarizability  $\beta_{M1}$ . At MAMI, measurements of polarizabilities of the proton are possible at the tagged photon beam line with the A2 setup and a major program of polarizability measurements is currently ongoing. The use of single polarization as well as double polarization variables indeed provides new and exciting opportunities for precision measurements, as will be discussed below.

Proton polarizabilities describe the response of the nucleon on an external electromagnetic field and provide fundamental information on the proton structure. We distinguish between the electric polarizability  $\alpha_{E1}$  and the magnetic polarizability  $\beta_{M1}$ . At higher orders also the four spin polarizabilities enter:  $\gamma_{E1E1}$ ,  $\gamma_{M1M1}$ ,  $\gamma_{E1M2}$ , and  $\gamma_{M1E2}$ . Fig.4 shows the current PDG [13] average of the electric and the magnetic polarizability along with several theoretical predictions from (heavy) baryon chiral perturbation theory, dispersion relations, and sum rules. Obviously, a precise measurement of the polarizabilities has the potential to distinguish between the various theoretical models.

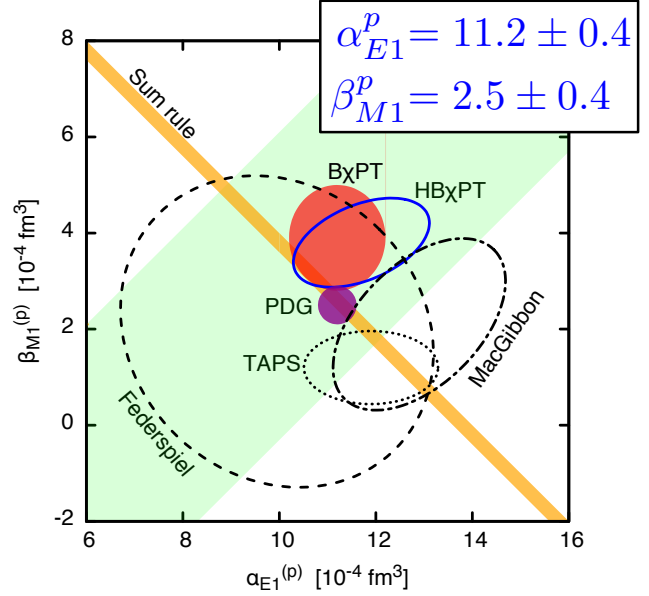


Fig. 4. PDG average and theoretical predictions for the scalar polarizabilities.

The A2 collaboration has carried out for the very first time a pilot experiment and has taken data on the cross section beam asymmetry  $\Sigma_3$ ,

$$\Sigma_3 = \frac{d\sigma_{\perp} - d\sigma_{\parallel}}{d\sigma_{\perp} + d\sigma_{\parallel}}, \quad (1)$$

in Compton scattering on protons below pion threshold. Linearly polarized photons, either parallel ( $\parallel$ ) or perpendicular ( $\perp$ ) to the scattering plane, are used for the measurement together with an unpolarized target. It was recently shown by the Mainz theory group [14] that in a model-independent framework  $\Sigma_3$  can be related to  $\beta_{M1}$ , since the term containing the electric polarizability is negligible at low photon energies.

Using an 883 MeV electron beam the degree of linear polarization reached about 75 % at photon energies around 130 MeV. Since the recoil proton has energies too low to be detected in the Crystal Ball, one neutral hit was required in the trigger. After subtraction of random events and background from empty target measurements, a clean missing mass distribution was obtained.

The data analysis is almost complete and a publication of this pilot experiment is in preparation. Clearly more data are necessary to improve the accuracy of  $\beta_{M1}$  significantly. The A2 collaboration plans to take additional data in 2016 to reduce the error on  $\beta_{M1}$  to a level of 10%. Such an increase in accuracy will also be possible due to the replacement of the photo multipliers for the focal plane of the tagging detector in addition to the recently installed new DAQ system.

In addition to the work related to the scalar polarizabilities, the A2 collaboration has also performed a mea-

surement of the spin polarizabilities by using the double polarization variable  $\Sigma_{2x}$ ,

$$\Sigma_{2x} = \frac{\sigma_{+x}^R - \sigma_{+x}^L}{\sigma_{+x}^R + \sigma_{+x}^L} = \frac{\sigma_{+x}^R - \sigma_{-x}^R}{\sigma_{+x}^R + \sigma_{-x}^R}, \quad (2)$$

where a right-handed ( $R$ ) or left-handed ( $L$ ) circularly polarized beam is scattered on a transversally ( $\pm x$ ) polarized target. The variable  $\Sigma_{2x}$  is particularly sensitive to the spin polarizability  $\gamma_{E1E1}$ , which is found to be  $\gamma_{E1E1} = (4.6 \pm 1.6) \times 10^{-4} \text{ fm}^3$ , see Ref.[15]. Again, with the improvements in the data taking rate for the A2 data taking, a significant improvement will be possible in the upcoming years.

### 3.2 Timelike electromagnetic form factor measurements of $\eta$ and $\eta'$ at A2

A new determination of the electromagnetic transition form factor (TFF) from the  $\eta \rightarrow e^+e^-\gamma$  Dalitz decay was carried out at A2/MAMI [17]. Experimentally, such a determination can be done by measuring the decay rate of  $\eta \rightarrow \gamma^*\gamma \rightarrow e^+e^-\gamma$  as a function of a dilepton invariant mass  $m_{ee} = q$  and by normalizing it to the partial decay width  $\Gamma(\eta \rightarrow \gamma\gamma)$ :

$$\frac{d\Gamma(\eta \rightarrow e^+e^-\gamma)}{q\Gamma(\eta \rightarrow \gamma\gamma)} = [QED] \cdot |F_\eta(q)|^2, \quad (3)$$

where  $F_\eta$  is the TFF of the  $\eta$  meson, and  $[QED]$  is the analytic QED expression of the decay ratio assuming structureless mesons, which depends on  $q$ , the mass of the  $\eta$  meson and the fine structure constant  $\alpha$  only. Assuming Vector Meson Dominance (VMD), TFFs are usually parametrized within a pole description:

$$F(q) = \frac{1}{1 - q^2/\Lambda^2}, \quad (4)$$

where  $\Lambda$  is the effective mass of the virtual vector mesons, with  $\Lambda^{-2}$  the FF slope at  $q^2=0$ .

The statistical accuracy achieved in this work surpasses all previous measurements of  $\eta \rightarrow e^+e^-\gamma$  and matches the NA60 result [16] based on  $\eta \rightarrow \mu^+\mu^-\gamma$  decays from peripheral In-In collisions. Compared to the former determination of the  $\eta$  TFF by the A2 collaboration [18] from 2011, an increase by more than one order of magnitude in statistics has been achieved. This was accomplished by an analysis of three times more data and the use of a kinematic-fit technique, which allowed for a higher selection efficiency and for exploiting the full  $\eta$  production range available at MAMI-C.

Our extracted slope parameter  $b = \Lambda^{-2} = (1.95 \pm 0.15_{\text{stat}} \pm 0.10_{\text{syst}}) \text{ GeV}^{-2}$  agrees within the uncertainties with the results from all recent measurements of the  $\eta$  TFF. The pole-approximation fit to the MAMI data shows almost perfect agreement with the model-independent calculation of Ref. [19], which was discussed

above in the theory section. The calculation by Ter-schlüsen and Leupold [20] and the dispersion theory calculation [21] by Hanhart et al. deviate slightly from the fit, but the statistical accuracy is still not sufficient to rule out any of the theoretical predictions, see Fig. 5.

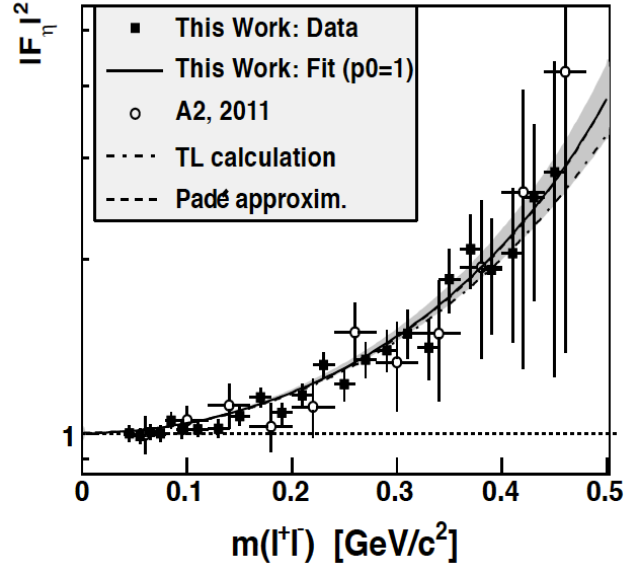


Fig. 5. Timelike  $\eta$  transition form factor measurement at A2/MAMI. Shown are two measurements from A2 (this work from 2013, 2011) together with a fit to the more recent measurement and two theoretical calculations (TL calculation, Padé approxim.), see text.

## 4 Search for the Dark Photon

Extra  $U(1)$  bosons – so-called dark photons,  $\gamma'$  – naturally appear in most string compactifications and in essentially any extensions of the SM. A prediction for the mass and the couplings is in general not possible. As a consequence, dedicated searches span a wide range of masses and couplings, exploiting very different experimental techniques (from atomic physics experiments to experiments at the LHC).

Recently, the focus of dark photon searches has moved to  $\gamma'$  masses in the MeV to GeV mass range. As Arkani-Hamed et al. in Ref. [22] have pointed out, dark photons in that mass range could be related to Dark Matter phenomena. In fact,  $\gamma'$  particles coupling to ordinary matter via so-called kinetic mixing give an elegant explanation for a number of astrophysical anomalies, such as e.g. the PAMELA/FERMI/AMS discovery of a positron excess in the cosmic ray flux.

Furthermore, it has been realized that dark photons with masses in the MeV to GeV range could also explain the presently seen deviation between the direct measurement of  $(g-2)_\mu$  and its Standard Model prediction. Given

the present size of the effect, a firm prediction for the dark photon parameter range (coupling parameter  $\epsilon$  versus Dark Photon mass  $m_{\gamma'}$ ) can be made [23].

#### 4.1 Dark Photon Search at A1

The experimental technique for the 2014 A1/MAMI measurement [24] is similar to the one used for the 2011 precursor experiment [25]. A high-intensity MAMI beam was scattered on a tantalum target. Electron-positron pairs are produced in QED processes, in which a virtual photon couples either in a timelike or a space like process to an  $e^+e^-$  pair. A dark photon could be produced by exchanging an ordinary photon by a dark photon. This would show up in the experiment as a bump over the QED background in the  $e^+e^-$  invariant mass spectrum.

In total, 22 kinematic settings were chosen with beam energies ranging from 180 MeV to 855 MeV. Depending on the setting, a 99.99% pure single foil  $^{181}\text{Ta}$  target or a stack of these foils was used. The result, which is shown in Fig. 6 in pink, was the most stringent limit below 400 MeV prior to a publication by BABAR [26].

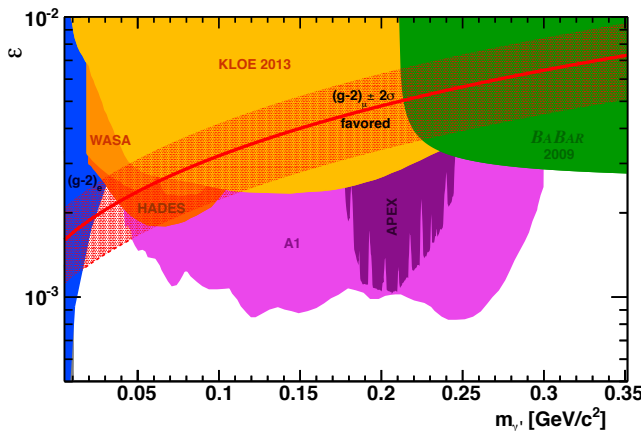


Fig. 6. Dark photon exclusion plot in the parameter range dark photon coupling ( $\epsilon$ ) versus dark photon mass ( $m_{\gamma'}$ ). The red (shaded) band shows the parameter range, in which a dark photon would explain the presently seen deviation between Standard Model prediction and direct measurement of  $(g-2)_\mu$ .

#### 4.2 Future Opportunities at MAGIX/MESA

The dual-arm high-resolution spectrometers in combination with a windowless internal gas target are ideally suited for the detection of low-momentum tracks and as such also for the dark photon search at low masses. A simulation has been carried out and it was found, that the MAGIX measurement will extend existing dark photon limits by almost an order of magnitude for masses below 50 MeV. A luminosity of  $10^{35}\text{cm}^{-2}\text{s}^{-1}$  has been assumed for the simulation, as also expected for a MESA

ERL beam of 1 mA in conjunction with the high-density gas jet target.

According to current plannings, the excellent resolution of the MAGIX spectrometers should also allow for a highly competitive dark photon search with an invisible decay of the dark photon into dark matter particles or neutrinos. This represents an extension of the Mainz dark photon program.

## 5 Conclusions

We have presented in this paper several typical measurements, which can be carried out at low-energy facilities as MAMI and at the future MESA facility. It is the low beam energy (or low energy transfer) together with world class luminosities, which allows for competitive measurements in the field of hadron and low-energy particle physics. In future, MESA will allow to extend this *low-energy frontier* further.

## References

- 1 H. Herminghaus, A. Feder, K. H. Kaiser, W. Manz and H. Von Der Schmitt, Nucl. Instrum. Meth. **138** (1976) 1; K. H. Kaiser *et al.*, Nucl. Instrum. Meth. A **593** (2008) 159.
- 2 K. I. Blomqvist *et al.*, Nucl. Instrum. Meth. A **403** (1998) 263.
- 3 J. C. McGeorge *et al.*, Eur. Phys. J. A **37** (2008) 129.
- 4 A. Thomas, Eur. Phys. J. ST **198** (2011) 171.
- 5 K. Aulenbacher, AIP Conf. Proc. **1563** (2013) 5.
- 6 N. Berger, these proceedings.
- 7 C. E. Carlson and M. Vanderhaeghen, arXiv:1109.3779.
- 8 H. Gao, these proceedings.
- 9 J. C. Bernauer *et al.* [A1 Collaboration], Phys. Rev. Lett. **105** (2010) 242001.
- 10 R. Pohl, R. Gilman, G. A. Miller and K. Pachucki, Ann. Rev. Nucl. Part. Sci. **63** (2013) 175.
- 11 K. Griffioen, C. Carlson and S. Maddox, arXiv:1509.06676.
- 12 M. O. Distler, T. Walcher and J. C. Bernauer, arXiv:1511.00479.
- 13 K. A. Olive *et al.* [Particle Data Group], Chin. Phys. C **38** (2014) 090001.
- 14 N. Krupina and V. Pascalutsa, Phys. Rev. Lett. **110** (2013) 26, 262001.
- 15 P. P. Martel *et al.* [A2 Collaboration], Phys. Rev. Lett. **114** (2015) 11, 112501.
- 16 R. Arnaldi *et al.* [NA60 Collaboration], Phys. Lett. B **677** (2009) 260.
- 17 P. Aguar-Bartolome *et al.* [A2 Collaboration], Phys. Rev. C **89**, 044608 (2014).
- 18 H. Berghäuser, V. Metag, A. Starostin, P. Aguar-Bartolome, L. K. Akasoy, J. R. M. Annand, H. J. Arends and K. Bantawa *et al.*, Phys. Lett. B **701** (2011) 562.
- 19 R. Escribano, P. Masjuan and P. Sanchez-Puertas, Phys. Rev. D **89** (2014) 034014.
- 20 C. Terschlusen and S. Leupold, Phys. Lett. B **691** (2010) 191.
- 21 C. Hanhart, A. Kupść, U.-G. Meißner, F. Stollenwerk, and A. Wirzba, Eur. Phys. J. C **73** (2013) 2668.
- 22 N. Arkani-Hamed, Phys. Rev. D **79**, 015014 (2009).
- 23 M. Pospelov, Phys. Rev. D **80**, 095002 (2009).
- 24 H. Merkel *et al.*, Phys. Rev. Lett. **112** (2014) 22, 221802.
- 25 H. Merkel *et al.* [A1 Collaboration], Phys. Rev. Lett. **106** (2011) 251802.
- 26 J. P. Lees *et al.* [BaBar Collaboration], Phys. Rev. Lett. **113** (2014) 20, 201801.